Development 138, 4801-4812 (2011) doi:10.1242/dev.070912
© 2011. Published by The Company of Biologists Ltd

ER71 directs mesodermal fate decisions during embryogenesis

Tara L. Rasmussen[1], Junghun Kweon[1], Mackenzie A. Diekmann[1], Fikru Belema-Bedada[1,2], Qingfeng Song[3], Kathy Bowlin[1], Xiaozhong Shi[1], Anwarul Ferdous[4], Tongbin Li[3], Michael Kyba[1], Joseph M. Metzger[1,2], Naoko Koyano-Nakagawa[1] and Daniel J. Garry[1,*]

SUMMARY

Er71 mutant embryos are nonviable and lack hematopoietic and endothelial lineages. To further define the functional role for ER71 in cell lineage decisions, we generated genetically modified mouse models. We engineered an *Er71-EYFP* transgenic mouse model by fusing the 3.9 kb *Er71* promoter to the *EYFP* reporter gene. Using FACS and transcriptional profiling, we examined the EYFP$^+$ population of cells in *Er71* mutant and wild-type littermates. In the absence of ER71, we observed an increase in the number of EYFP-expressing cells, increased expression of the cardiac molecular program and decreased expression of the hemato-endothelial program, as compared with wild-type littermate controls. We also generated a novel *Er71-Cre* transgenic mouse model using the same 3.9 kb *Er71* promoter. Genetic fate-mapping studies revealed that the ER71-expressing cells give rise to the hematopoietic and endothelial lineages in the wild-type background. In the absence of ER71, these cell populations contributed to alternative mesodermal lineages, including the cardiac lineage. To extend these analyses, we used an inducible embryonic stem/embryoid body system and observed that ER71 overexpression repressed cardiogenesis. Together, these studies identify ER71 as a critical regulator of mesodermal fate decisions that acts to specify the hematopoietic and endothelial lineages at the expense of cardiac lineages. This enhances our understanding of the mechanisms that govern mesodermal fate decisions early during embryogenesis.

KEY WORDS: Transgenesis, *Er71* (*Etv2*) knockout, Mouse

INTRODUCTION

Transcriptional networks, signaling cascades, microRNAs and other factors coordinately regulate stem and progenitor cell populations to give rise to the mesodermal lineages (Davis and Zur Nieden, 2008; Ivey et al., 2008; Omelyanchuk et al., 2009; Park et al., 1998). During embryogenesis, a set of anterior progenitors coalesce to form the heart. These progenitors, along with the blood and vasculature, comprise the circulatory system, which is the first organ system to develop in mouse and human. Disruption or elimination of any one of these lineages results in early embryonic lethality. However, the factors that regulate the co-emergence of these lineages from the mesodermal progenitor pools are incompletely defined.

Recent studies have identified a multipotent progenitor cell population that is capable of giving rise to the cardiomyocyte and endothelial lineages during embryogenesis (Kattman et al., 2006; Moretti et al., 2006; Wu et al., 2006). Although these multipotent progenitors have been identified based on the expression of Flk1 (also known as Kdr), Nkx2-5 and Isl1, the transcriptional networks that govern the fate of these progenitors are unknown. These and other studies emphasized the plasticity and context dependence of regulatory cascades in the progenitor cell populations. For example, our previous studies demonstrated that Nkx2-5 has a dual transcriptional regulatory role in the promotion of the cardiac lineage and suppression of the hematopoietic lineage (Caprioli et al., 2011). In this fashion, we proposed that the stoichiometry of regulatory transcription factors and interacting factors could dynamically regulate the fate of progenitors. Definition of additional networks and signaling pathways that promote and suppress the fate of distinct lineages that arise from multipotent progenitors will enhance our mechanistic understanding of their developmental potential.

Ets-related protein 71 (ER71; Etv2) is a member of the Ets transcription factor family that we and others have shown to be essential for formation of the endothelial and hematopoietic lineages (De Val et al., 2008; Ferdous et al., 2009; Lee et al., 2008). *Er71* can be induced by BMP, Wnt and Notch signals to promote hematopoiesis (Lee et al., 2008) and synergizes with FoxC2 to regulate the endothelial program by directly targeting Scl (also known as Tal1), Notch4, Cdh5 and Tie2 (also known as Tek) (De Val et al., 2008; Ferdous et al., 2009; Lee et al., 2008). In *Er71* mutant mouse embryos, there is a complete lack of hematopoietic and endothelial lineages and the embryos are nonviable by embryonic day (E) 9.5 (Ferdous et al., 2009; Lee et al., 2008). Analysis of the *Er71* mutant embryos revealed no differences in cellular proliferation or cellular apoptosis compared with age-matched wild-type littermates (Ferdous et al., 2009). These results raised the question of whether the hematopoietic and endothelial precursors are still present but unable to differentiate to hemato-endothelial lineages, whether they had been redirected towards other lineages or whether these cells never arose during development.

[1]Lillehei Heart Institute, University of Minnesota, Minneapolis, MN 55455, USA. [2]Department of Integrative Biology & Physiology, Medical School, University of Minnesota, Minneapolis, MN 55455, USA. [3]Biolead.org Research Group, LC Sciences, Houston, TX 77054, USA. [4]University of Texas Southwestern Medical Center, Dallas, TX 75244, USA.

*Author for correspondence (garry@umn.edu)

Accepted 5 September 2011

In the present study, we have dissected ER71-mediated mechanisms that govern fate determination during murine embryogenesis. We have generated a novel transgenic mouse model in which the 3.9 kb *Er71* promoter drives the *EYFP* reporter (*Er71-EYFP*), and crossed it into the *Er71* wild-type and mutant backgrounds. This strategy facilitates the isolation and characterization of cells that would normally express ER71 from *Er71* mutant embryos. In the absence of ER71, we observed the conversion of cells that would normally give rise to lateral plate mesoderm into cells that produce paraxial and cardiac mesoderm. Furthermore, ER71 overexpression in vitro using an inducible embryonic stem cell/embryoid body system demonstrated decreased cardiogenic potential. Collectively, these data complement and extend our understanding of the functional role of ER71 to differentially promote mesodermal fate decisions during embryogenesis.

MATERIALS AND METHODS

Generation of transgenic mice

The 3.9 kb *Er71* promoter (Ferdous et al., 2009), which harbors the modules necessary to direct the temporal and spatial expression of ER71, was cloned into the pEYFP-1 vector (BD Biosciences) and into a promoterless pBS-Cre-pA vector to generate the ER71-EYFP and ER71-Cre constructs, respectively. Transgenic animals were generated at the University of Minnesota Mouse Genetics Laboratory using standard methods. Transgenic mice were screened for DNA integration by PCR. Expression analysis of ER71-EYFP lines was performed by examining E7.0-9.5 embryos resulting from timed matings to wild-type CD1 mice (Charles River). We also analyzed E11.0 and postnatal day (P) 3 offspring of timed matings of the ER71-Cre lines and the Rosa-EYFP line (Jackson Labs 006148). Founder mouse lines were crossed to the *Er71* heterozygotes previously described (Ferdous et al., 2009). In all cases, at least three transgenic lines were examined to confirm similar temporal and spatial expression patterns. All mice were maintained at the University of Minnesota under protocols approved by the Institutional Animal Care and Use Committee and Research Animal Resources.

FACS analysis

Embryos from timed pregnant females were harvested at specified stages. Embryos were separated from yolk sacs, which were used for genotyping, and imaged on a Zeiss Axio Observer Z1 inverted microscope prior to dissociation. Embryos between E7.5 and E9.5 were digested in 30-50 μl 0.25% trypsin plus EDTA at 37°C. Digestion was arrested with 500 μl DMEM containing 10% fetal bovine serum (FBS). Cells were pelleted at 4°C (1600 ***g***), resuspended in PBS and passed through a 70 μm cell strainer. Cells were incubated with antibody cocktails for 30 minutes, washed, and resuspended in PBS. Cells were analyzed or sorted using a FACSAria (BD Biosciences). Various combinations of antibodies (1:1000) were used, including Flk1-APC (eBiosciences 17-5821), Pdgfra-PE (eBiosciences 12-1401), CD31-PECy7 (eBiosciences 25-0311), CD34-PE (BD Pharmingen 551387), cKit-APC (eBiosciences 17-1171), CD41-PECy7 (eBiosciences 25-0411), CD45-PE (BD Pharmingen 553081), CD45-PECy7 (eBiosciences 25-0451-81), and Ter119-APC (BD Pharmingen 561033) antibodies.

Transcriptome analysis

Total RNA was isolated from 1000-5000 FACS sorted cells in TRIzol (Invitrogen) using the PureLink Mini RNA system (Ambion). RNA was subjected to two rounds of amplification using the MessageAmp II aRNA Amplification Kit (Ambion) and then labeled using the MessageAmp II-Biotin Enhanced Kit (Ambion) according to manufacturer's protocols. Amplified RNAs were hybridized to Affymetrix mouse 430 2.0 full genome array chips at the BioMedical Genomics Center of the University of Minnesota. The CEL data files produced from Affymetrix array experiments were processed using the affy package included in Bioconductor. The robust multi-array (RMA) method (Irizarry et al., 2003) was used to perform data normalization, background correction and expression quantification. The limma package (Smyth, 2005) was used to identify differentially expressed genes by ANOVA analysis, and false discovery rate (FDR) values were calculated using the Benjamini-Hochberg method (Benjamini and Hochberg, 1995). Average linkage hierarchical clustering analysis was performed using the cluster program (de Hoon et al., 2004), with uncentered Pearson's correlation coefficient used to define pairwise similarity in gene expression. Genes annotated with the gene ontology (GO) term 'heart development' (GO:0007507) were downloaded with AmiGO tool (Carbon et al., 2009) and used in producing the heatmaps. Microarray data is accessible in Gene Expression Omnibus (series GSE32223).

Quantitative RT-PCR

Total RNA was isolated from 1000-5000 FACS sorted cells or embryoid body cells in TRIzol (Invitrogen) using the PureLink Mini RNA system. RNA from FACS sorted cells was subjected to two rounds of amplification as described above, but left unlabeled. cDNA was made using random hexamers and transcript levels were determined using VIC-labeled (*Gapdh*, 4352339E) or FAM-labeled (*Er71*, mm01176581_g1; *Scl*, mm01187033_m1; *Cdh5*, mm00486938_m1; *Gata4*, mm00484689_m1; *Tbx5*, mm00803518_m1; *Tnnt2*, mm00441922_m1) TaqMan probe sets (Applied Biosystems).

Embryoid body differentiation and ER71 overexpression

Doxycycline-dependent ER71-overexpressing mouse embryonic stem (mES) cells were generated using an inducible cassette exchange strategy (Iacovino et al., 2009). In this system, ER71 tagged with a C-terminal HA epitope was overexpressed in response to 0.5 μg doxycycline. To mimic early embryonic development, the mES cells were differentiated into embryoid bodies (EBs) using mesodermal differentiation media [1.5% FBS (Stem Cell Technology), 1× penicillin/streptomycin, 1× GlutaMAX (Gibco), 100 μg/ml Fe-saturated transferrin, 450 mM monothioglycerol, 50 μg/ml ascorbic acid in IMDM (Invitrogen)] (Kennedy et al., 1997). ER71 was induced on day 3 after initiating differentiation and maintained through day 10 by supplementing the differentiation media with doxycycline. On day 10, we fixed the EBs with 4% paraformaldehyde (PFA) and prepared cryosections. We stained adjacent sections with Hematoxylin and Eosin using a standard protocol and performed immunostaining with mouse anti-TnT serum (1:200, DSHB clone CT3). We assayed the TnT-expressing area of each EB using ImageJ software (NIH) and calculated the ratio of the positive area to the total area from 33 sections of uninduced EBs and 42 sections of induced EBs. EBs were placed on laminin-coated coverslips and stimulated at 1 Hz. Edge detection (Ionoptix, Milton, MA, USA) was used to measure contractility of intact EBs.

Immunohistochemical analysis

Stage-specific embryos were harvested from time-mated pregnant females. For paraffin sectioning, embryos were fixed for 4-8 hours at 4°C in 4% PFA and embedded. For cryosectioning, embryos were fixed for 1 hour at 4°C in 4% PFA and embedded in OCT compound (Sakura). Sections were blocked with immunohistochemical diluent (2% normal donkey serum, 1% bovine serum albumin, 0.3% Triton X-100, 0.02% sodium azide in PBS, pH 7.3) at room temperature and incubated overnight at 4°C with primary antibodies, including chicken anti-GFP (1:500, Abcam ab13970), rabbit anti-desmin (1:200, Novus Biologicals NB120-15200), rat anti-Tie2 (1:100, eBiosciences 13-5987-81), rat anti-Pdgfra (1:200, eBiosciences 12-1401-81), goat anti-Nkx2-5 (1:500, Santa Cruz SC-8697) and anti-CD41 (1:100, BD Pharmingen 550274), anti-Cdh5 (1:100, BD Pharmingen 55289), anti-CD31 (1:200, BD Pharmingen 550274), anti-Gata1 (1:100, Santa Cruz SC 265X) and anti-troponin T (1:200, DSHB CT3) sera. Slides were washed and incubated with combinations of secondary antibodies (1:200) including anti-chicken Dylight 488, anti-rabbit Cy3, anti-mouse Cy3, anti-rat Cy3 and anti-goat Dylight 549 (Jackson ImmunoResearch Laboratories). Results were imaged on a Zeiss Axio Imager M1 upright microscope or a Zeiss LSM 510 Meta confocal microscope.

Statistical analysis

Data represent the average of at least three replicates and s.e.m. Significance was tested by the Kruskal-Wallis test with the Dunn multiple comparison test for more than two groups; for example, when comparing

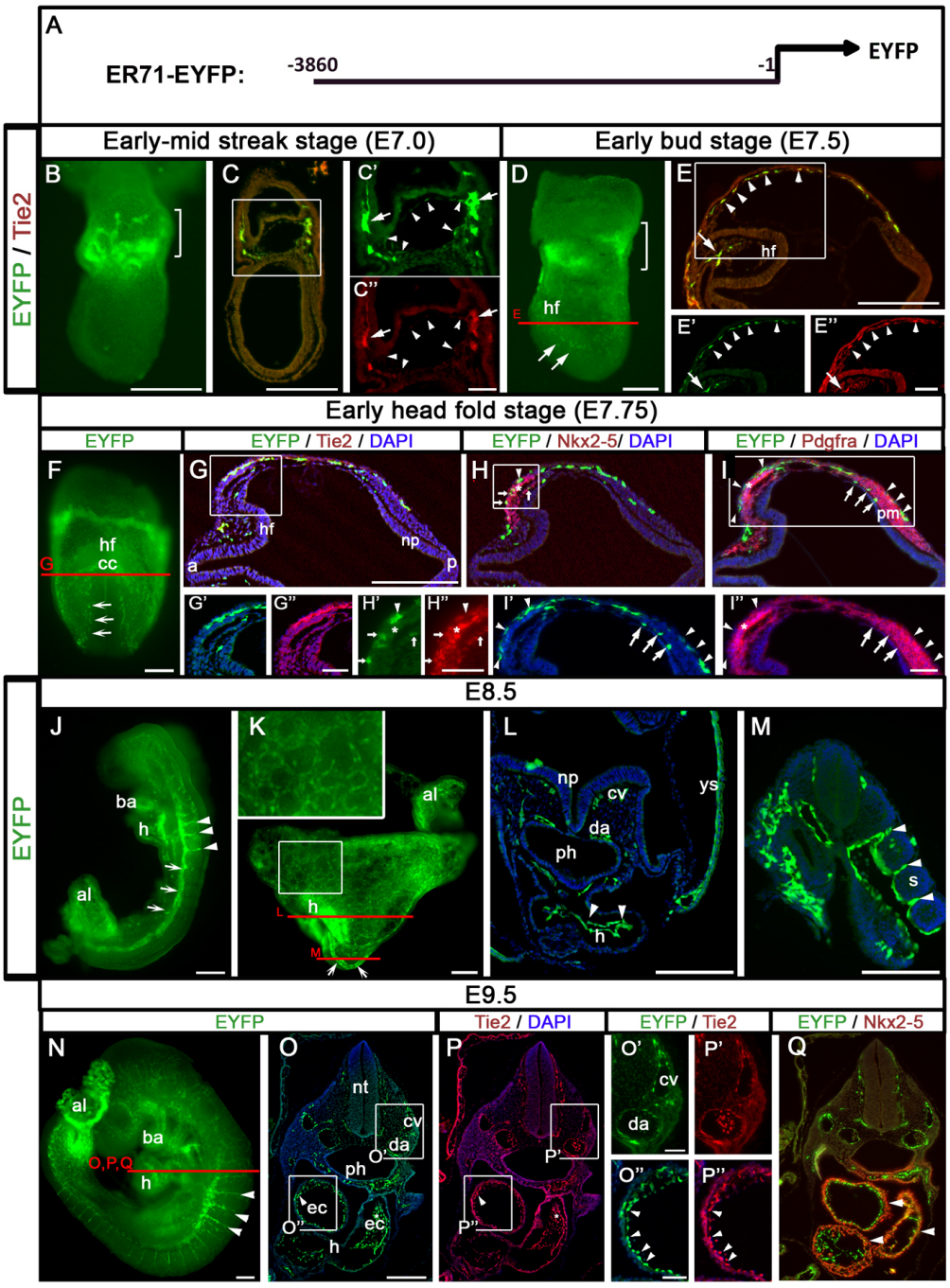

Fig. 1. The transgenic ER71-EYFP reporter is expressed during embryogenesis. (**A**) The transgenic *Er71-EYFP* construct used in these analysis. (**B-Q**) Expression analysis of mouse embryos between E7.0 and E9.5. EYFP protein fluorescence (green) is shown in whole-mount images (B,D,F,J,K,N). Sections were stained with anti-GFP (green), anti-Tie2 (red), anti-Nkx2-5 (red) or anti-Pdgfra (red) antibody as indicated. DAPI nuclear staining is shown in blue. Yellow indicates overlap of green and red channels. (B-C″) Early to mid streak stage, (D-E″) early bud stage, (F-I″) early head-fold stage, (J-M) E8.5, (N-Q) E9.5; embryos were staged according to Downs and Davies (Downs and Davies, 1993). Boxed regions are shown at higher magnification; planes of sections are indicated. See first section of the Results for a description of arrows, arrowheads and other labels. al, allantois; ba, branchial arch; bi, blood island; cc, cardiac crescent; cv, cardinal vein; da, dorsal artery; ec, endocardium; h, heart; hf, head fold; np, neural plate; nt, neural tube; ph, pharynx; pm, paraxial mesoderm; s, somite; ys, yolk sac. Scale bars: 200 μm; 50 μm in enlargements.

wild type, heterozygous and homozygous mutants. Significance was tested by the Mann-Whitney U test for two groups. Analyses were performed using Prism5 software (GraphPad).

RESULTS

Expression analysis of the ER71-EYFP reporter

Initial analysis of ER71 expression in the developing mouse embryo was reported previously (Ferdous et al., 2009; Lee et al., 2008). To further examine its potential role in cardiovascular development, we performed a detailed expression analysis of ER71 from E7.0 to E9.5, when *Er71* mRNA is expressed (Ferdous et al., 2009). None of the commercially available ER71 antibodies detected the endogenous protein, so we utilized an *Er71* transgenic mouse driving an enhanced yellow fluorescent protein (*EYFP*) reporter. The 3.9 kb region upstream of the *Er71* transcription start site was fused to the *EYFP* reporter (Fig. 1A). This promoter fragment was previously shown to drive reporter expression that recapitulated endogenous ER71 expression (Ferdous et al., 2009). Four founder lines were generated with offspring embryos that showed the same expression pattern.

To examine the expression pattern of the EYFP reporter, we compared its expression to that of the angiopoietin 1 receptor Tie2, which marks endothelial cells in mice and humans (Dumont et al., 1992; Sarb et al., 2010; Schlaeger et al., 1997; Schnurch and Risau, 1993). The EYFP reporter (representing ER71 expression) was expressed as early as the early to mid gastrulation stage (E7.0; Fig. 1B, bracket). At this stage, reporter expression was limited to the extra-embryonic mesoderm (Fig. 1C) and showed co-expression

with Tie2 in the primitive blood islands (Fig. 1C′,C″, arrows) (Ema et al., 2006b). EYFP was also weakly expressed in the mesothelial layer of the yolk sac, but Tie2 was absent in this non-endothelial cell population (Fig. 1C′,C″, arrowheads). At E7.5, continued expression of the EYFP reporter was observed in the extra-embryonic mesoderm (Fig. 1D, bracket). In addition, scattered EYFP$^+$ cells were observed in the lateral plate mesoderm (Fig. 1D, arrows). Transverse sections showed that these scattered cells co-expressed Tie2 and most likely represent endothelial progenitors (Fig. 1E,E′,E″), although Tie2 expression has also been identified in a subset of cells committed to the hematopoietic lineage (Kisanuki et al., 2001; Li et al., 2005).

At E7.75, the EYFP signal localized to discrete structures including the cardiac crescent and the progenitors of the dorsal aortae (Fig. 1F, cc, arrows). We examined the expression in the cardiac crescent and paraxial mesoderm in detail using Nkx2-5 and Pdgfra antibodies (Fig. 1G-I). We observed that the EYFP signal overlapped extensively with Tie2 within the cardiac crescent (Fig. 1G′,G″). These EYFP$^+$ cells are presumably endocardial progenitors (Misfeldt et al., 2009). By contrast, EYFP$^+$ cells either weakly expressed or did not express Nkx2-5 (Fig. 1H′,H″, arrows and arrowheads, respectively). We did not observe strong co-expression of Nkx2-5 and EYFP. Pdgfra is strongly expressed in paraxial mesoderm and cardiac mesoderm (Fig. 1I, pm and asterisk). Double immunohistochemical labeling of EYFP and Pdgfra demonstrated that most cells either did not co-express these markers or weakly expressed Pdgfra (Fig. 1I,I′,I″, arrowheads and arrows, respectively), which is consistent with previous reports that the hemogenic lineage is segregated from the paraxial mesoderm early during gastrulation (Kataoka et al., 1997; Takakura et al., 1997).

At E8.5 and E9.5, we observed localization of the EYFP signal to vascular structures throughout the embryo proper (Fig. 1J,N; arrows point to the dorsal aorta and arrowheads indicate intersomitic vessels) and yolk sac (Fig. 1K). Transverse sections of the embryos (Fig. 1L,M,O,P) showed localized expression in the vessel structures including dorsal aorta, cardinal vein, intersomitic vessels (arrowheads in Fig. 1M) and the endocardium (arrowheads in Fig. 1L). The expression of EYFP largely overlapped with that of Tie2, indicating that the *Er71* promoter is active in early embryonic endothelial and hematopoietic cells (Fig. 1O-P″). We also observed that EYFP was co-expressed with the hematopoietic transcription factor Gata1, the cell surface marker of hematopoietic progenitors CD41 (also known as Itga2b), the marker of hematopoietic and endothelial lineages Cdh5, and with the primarily endothelium-specific cell surface marker CD31 (also known as Pecam1) (supplementary material Fig. S1). By E9.5, Nkx2-5 was localized to the myocardial layer of the heart and did not overlap with EYFP expression (Fig. 1Q, arrowheads; compare with 1O).

Reporter expression is mislocalized in the *Er71* mutant

In the *Er71* mutant, the hematopoietic and endothelial lineages are absent. However, no changes were observed in cellular proliferation or apoptosis in the *Er71* mutant embryo (Ferdous et al., 2009). Therefore, we crossed the ER71-EYFP reporter line into the *Er71* mutant background to define and characterize the cells that should give rise to these lineages (Fig. 2). In the E7.75 wild-type embryo, EYFP expression was observed throughout the cardiac crescent, the dorsal aortae and the extra-embryonic mesoderm (Fig. 2A). By contrast, in the E7.75 mutant embryo the expression pattern was less definitive. EYFP-positive cells were found in the extra-embryonic tissue; however, expression of EYFP within the embryo proper was mislocalized (Fig. 2B, arrow). EYFP expression appeared diffuse throughout the cardiac crescent (Fig. 2B, asterisk). In the wild-type embryo at E8.0, EYFP expression was observed specifically in the dorsal aortae, but not on the periphery of the embryo (Fig. 2C, arrowheads). EYFP expression was also observed in the presumptive endocardium within the linear heart tube (Fig. 2C). By contrast, the *Er71* mutant embryos expressed EYFP only at the periphery of the embryo, which is likely to represent paraxial mesoderm (Fig. 2D). Immunohistochemical analysis of ER71-EYFP and Pdgfra, a marker of paraxial mesoderm, expression in E8.5 wild-type and mutant embryos demonstrates that EYFP-positive cells are interspersed within the Pdgfra-positive mesoderm (supplementary material Fig. S2). FACS profiling showed that the frequency of EYFP$^+$ cells was increased in the *Er71* mutant compared with the wild-type control at E8.0 (Fig. 2G-I), but not at E7.75 (Fig. 2E,F,I). The apparent increase in the percentage of EYFP$^+$ cells could be due to a reduction in the total number of cells without a change in the number of EYFP$^+$ cells, as cell viability can be reduced by a lack of vascularization. However, we ruled out this possibility as we also observed a doubling in the absolute number of EYFP$^+$ cells in E8.0 *Er71* mutant embryos as compared with wild-type littermates (Fig. 2J).

These analyses demonstrated that cells that expressed the ER71 reporter were not only present in the *Er71* mutant embryo, but were also expanded in number. Since the *Er71* mutant embryo lacks differentiated endothelial and hematopoietic lineages, we examined whether these EYFP$^+$ cells were arrested progenitors or cells redirected to other lineages. We used FACS analysis to examine the cell surface markers of the EYFP$^+$ cells in the *Er71* mutant and wild-type backgrounds. Previous studies have established that Pdgfra is expressed in the primitive streak at E7.0, but is restricted to the paraxial mesoderm at the early head-fold stages (Takakura et al., 1997). Flk1 is expressed more broadly in mesodermal precursors (Ema et al., 2006a; Motoike et al., 2003), including the posterior portion of the primitive streak. Flk1$^+$/Pdgfra$^-$ cells mark lateral plate mesoderm that will give rise to the endothelial and hematopoietic lineages and Flk1$^-$/Pdgfra$^+$ cells mark the paraxial mesoderm. Flk1 and Pdgfra are known to be co-expressed in the cardiac crescent (Kataoka et al., 1997) and in cardiac progenitors of embryoid bodies (EBs) (Bondue et al., 2011; Kattman et al., 2006). In the present study, the frequency of Flk1$^+$ cells within the EYFP$^+$ population was significantly reduced at E7.75 and E8.0 (Fig. 3A,B,D,F). CD41 (Fig. 3D,E) and CD34 (Fig. 3E,F) expression was essentially absent at E8.0 in the EYFP$^+$ cells of the *Er71* mutant. These results show that the lateral plate mesoderm lineage and its derivatives, i.e. the hematopoietic and endothelial lineages, are reduced in the *Er71* mutant.

In order to assess which lineages are expressing ER71-EYFP, we analyzed the EYFP$^+$ cells using Flk1 and Pdgfra antibodies. Concurrent with the decrease of Flk1 expression at E7.75 and E8.0, we observed an increase in the frequency of EYFP$^+$ cells that express Pdgfra (Fig. 3A,B). This correlated with a significant increase of Pdgfra single-positive cells at E7.75 and a significant increase of Flk1$^+$/Pdgfra$^+$ cells at E8.0 (Fig. 3A,C). There was also a trend toward expansion of Pdgfra single-positive cells within the EYFP$^+$ population at E8.0 (Fig. 3A,C). To support these observations, we used immunohistochemistry to analyze the EYFP expression patterns. In wild-type embryos, EYFP expression is distinct from Pdgfra$^+$ paraxial mesoderm. A select number of EYFP-positive cells are found within this region; however, these cells are Pdgfra$^-$ (supplementary material Fig. S2A,B). In mutant

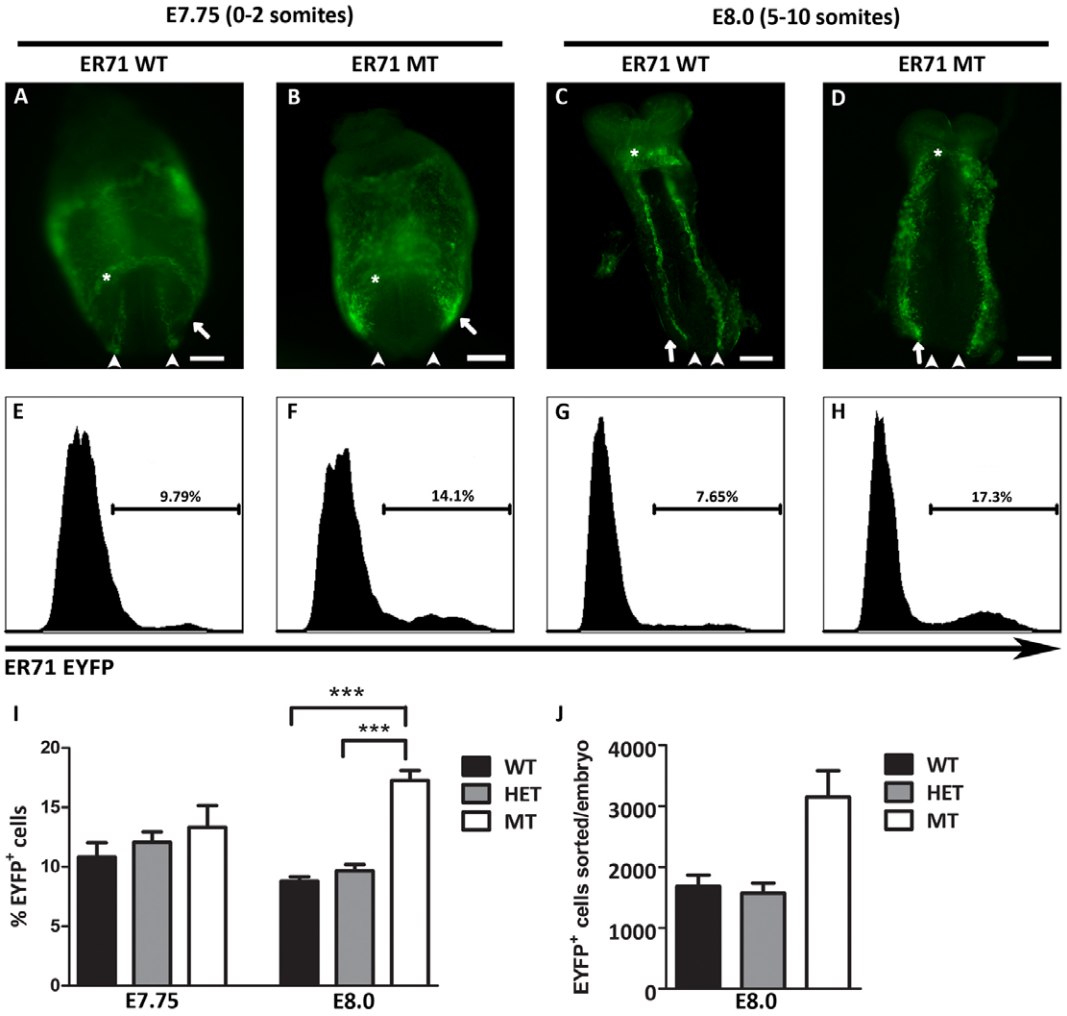

Fig. 2. The ER71 reporter is misexpressed in *Er71* mutant embryos. (**A-H**) EYFP expression in *Er71* wild type (A,C,E,G) and mutant (B,D,F,H) mouse embryos at E7.75 (A,B,E,F) and E8.0 (C,D,G,H). Asterisks indicate the cardiac crescent (A,B) or forming linear heart tube (C,D). Arrowheads indicate the bilateral dorsal aortae (C,D) or its progenitors (A,B). Arrows point to regions in which EYFP is misexpressed in the mutant (A-D). Representative FACS profiles of individual embryos (E-H) show the percentage of EYFP positive cells per embryo. Scale bars: 200 μm. (**I**) The percentage of EYFP$^+$ cells for all experiments. (**J**) The average number of EYFP$^+$ cells sorted per embryo. WT, wild type; HET, *Er71* heterozygote; MT, homozygous *Er71* mutant. ***, $P<0.001$. Error bars indicate s.e.m.

embryos, many EYFP$^+$ cells are found within the Pdgfra$^+$ paraxial mesoderm. Some of these cells are double positive for EYFP and Pdgfra (supplementary material Fig. S2C,D). Likewise, in wild-type embryos, EYFP expression is distinct from troponin T (TnT)$^+$ cardiomyocytes (supplementary material Fig. S2E). However, in mutant embryos double-positive cells are found (supplementary material Fig. S2F,G, arrows). One interpretation of these data is that, in the absence of ER71, the EYFP$^+$ progenitor cells differentiate towards the paraxial (Flk1$^-$/Pdgfra$^+$) and cardiac mesodermal (Flk1$^+$/Pdgfra$^+$) lineages at the expense of the lateral plate/hemangiogenic mesodermal (Flk1$^+$/Pdgfra$^-$) lineage.

An alternative explanation of these results is that EYFP is expressed ectopically in cardiac (Flk1$^+$/Pdgfra$^+$) and paraxial (Flk1$^-$/Pdgfra$^+$) mesodermal populations in the absence of ER71. If this were the case, we would expect the cardiac and paraxial mesodermal populations within the EYFP$^-$ gate to decrease in the mutant embryos because these cells expressed EYFP and would be included in the EYFP$^+$ gate. Furthermore, we would expect no change in the overall representation of these markers in the unfractionated (the sum of EYFP$^+$ and EYFP$^-$) gate. To examine this possibility, we analyzed unfractionated cells from the whole embryo as well as EYFP$^-$ fractionated cells. In the EYFP$^-$ fraction no changes were observed in the mesodermal populations at E7.75 (supplementary material Fig. S3C,D) and E8.0 (supplementary material Fig. S3G,H). Analysis of the whole population (the sum of EYFP$^-$ and EYFP$^+$ gates) showed no change in cardiac or paraxial populations at E7.75 (supplementary material Fig. S3A,B); but at E8.0, we observed a small, but reproducible, increase in the cardiac mesoderm (Flk1$^+$/Pdgfra$^+$) (supplementary material Fig. S3E,F). We predict that the increase in cardiac mesoderm in the whole embryo is small because the EYFP$^+$ population is a minor fraction of the entire embryo.

Collectively, our results support the model that, in the *Er71* mutant background, EYFP$^+$ cells differentiate to the cardiac mesoderm lineage and contribute to the increase in cardiac mesoderm (Flk1$^+$/Pdgfra$^+$) markers, rather than cardiomyocytes or cardiac progenitors ectopically expressing EYFP.

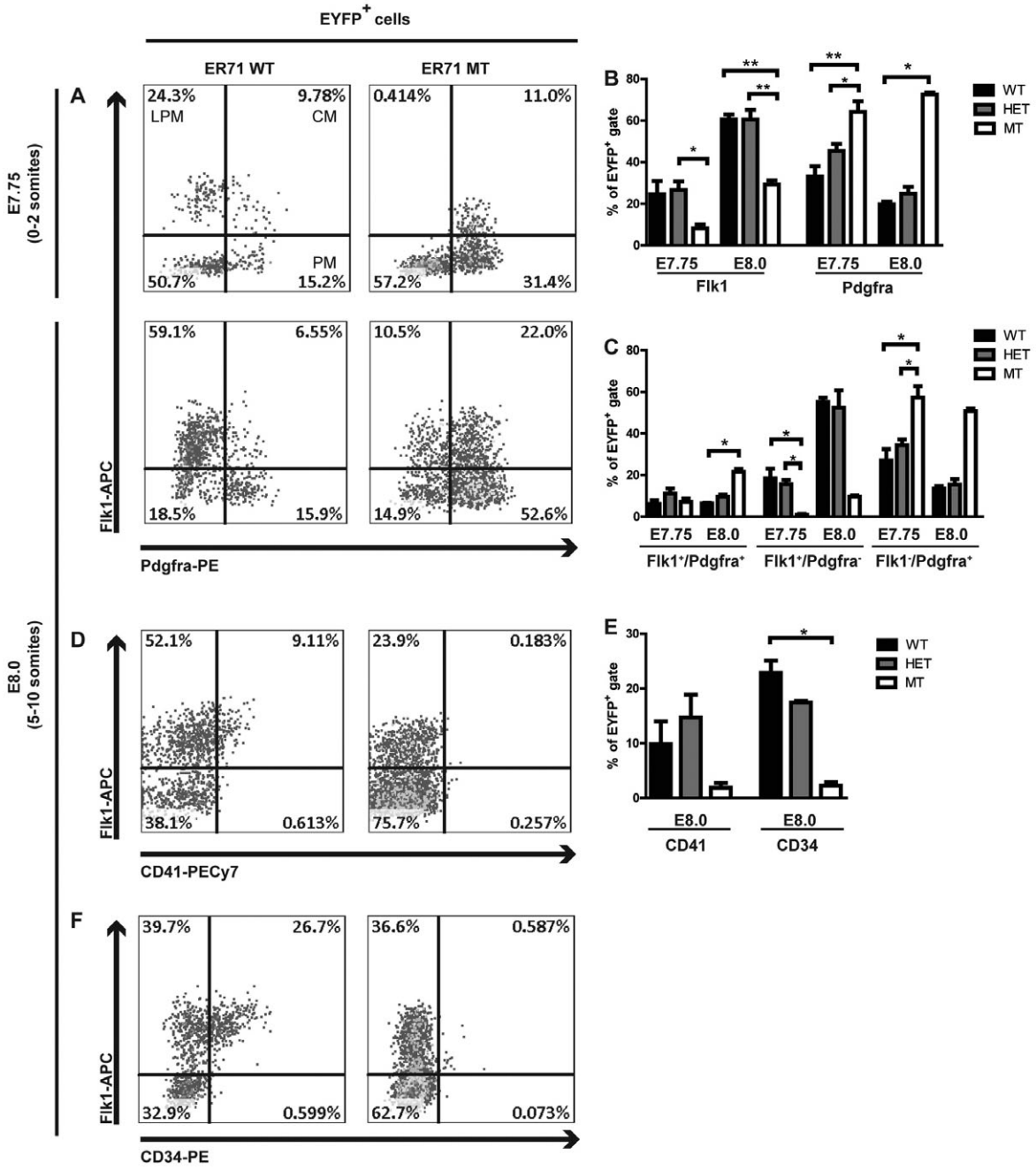

Fig. 3. ER71-EYFP$^+$ cells in *Er71* mutant mouse embryos lack markers of hematopoietic progenitors in exchange for those of other mesodermal lineages. (**A**) Using fluorophore-conjugated antibodies and FACS analysis, we observed an enrichment of Pdgfra$^+$ cells in ER71-EYFP$^+$ mutant cells at E7.75 and E8.0. (**B**,**C**) Summary of multiple experiments comparing individual fluorophores Flk1 and Pdgfra (B), and combinations of Flk1 and Pdgfra (C). (**D**,**F**) Hematopoietic progenitor cell surface markers are not expressed in the embryo proper at E7.75, but there is a significant reduction in CD41 (D) and CD34 (F) at E8.0. (**E**) Summary of multiple experiments comparing hemogenic and endothelial markers CD41 and CD34. **, $P<0.01$; *, $P<0.05$. Error bars indicate s.e.m. LPM, lateral plate mesoderm; CM, cardiac mesoderm; PM, paraxial mesoderm.

Cardiac and skeletal muscle genes are upregulated in ER71-EYFP$^+$ cells in *Er71* mutant embryos

To further examine whether the EYFP$^+$ cells in the absence of ER71 were redirected to other mesodermal lineages, we performed a transcriptome analysis. We used an Affymetrix microarray platform and examined the EYFP-positive and EYFP-negative cells from wild-type and *Er71* mutant littermate embryos. Genes that were significantly dysregulated were filtered based on the false discovery rate (FDR<0.01 for EYFP$^+$ versus EYFP$^-$; FDR<0.35 for wild type versus mutant; FDR<0.01 for the interaction between these two variables). Clustering analysis was carried out subsequently (Fig. 4A). Interestingly, there were no transcripts that showed differential expression between EYFP$^-$ populations in the *Er71* wild-type and mutant backgrounds. Also, the cluster analysis was unable to resolve differences between the EYFP$^-$ populations

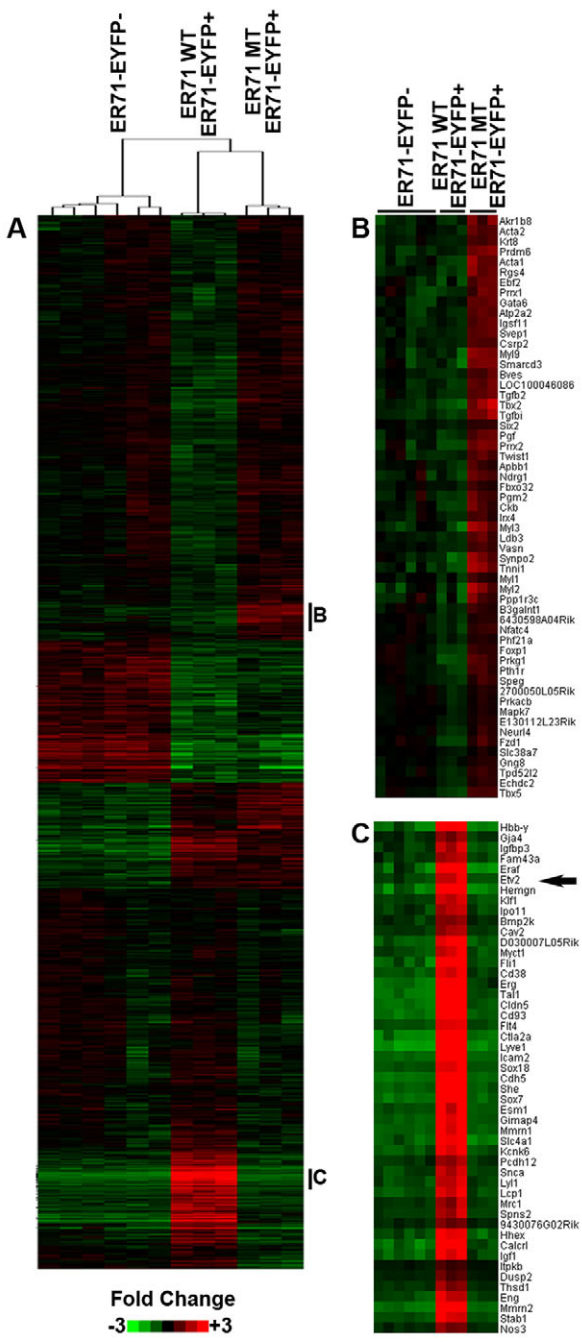

Fig. 4. Transcriptome analysis reveals that hemato-endothelial and cardiac lineages are dysregulated in the *Er71* mutant embryo. Transcriptome analysis was performed on EYFP$^+$ and EYFP$^-$ cells sorted from wild-type and *Er71* mutant littermate mouse embryos. (**A**) Clustering analysis shows that wild-type and mutant EYFP$^-$ cells are indistinguishable, whereas EYFP$^+$ cells from wild-type and mutant embryos show distinct gene expression profiles. (**B**) Transcripts upregulated in the EYFP$^+$ mutant progenitors include cardiac and skeletal muscle genes. (**C**) Downregulated transcripts in the *Er71* mutant background include hemato-endothelial transcripts, including *Er71* (*Etv2*) (arrow).

(Fig. 4A). These transcriptome results for the EYFP$^-$ cells support the notion that EYFP is not being expressed ectopically. Furthermore, this indicated that there were no significant non-cell-autonomous effects on gene expression resulting from the lack of ER71 at this time point.

Within the EYFP$^+$ populations, the *Er71* mutant and wild-type cells were significantly different (Fig. 4A). A large number of hematopoietic and endothelial transcripts were decreased in expression between *Er71* wild-type EYFP$^+$ and *Er71* mutant EYFP$^+$ cells (Fig. 4C). Importantly, ER71 expression was restricted to the EYFP$^+$ cells in the wild-type background (Fig. 4C, arrow), confirming that the *Er71-EYFP* transgenic model reflects endogenous ER71 expression. Other transcripts that were downregulated in the mutant EYFP$^+$ cells compared with the *Er71* wild-type EYFP$^+$ cells included endothelial and hematopoietic transcripts such as *Hbb-y*, *Fli1*, *Erg*, *Tal1*, *Cldn5*, *Cd93*, *Sox18*, *Cdh5*, *Sox7*, *Mmrn1*, *Eng* and *Nos3* (Fig. 4C). These data indicated that the EYFP reporter-positive cells contributed to the endothelial and hematopoietic lineages and did not express markers of those lineages in the absence of ER71, consistent with the previously described phenotypes (Ferdous et al., 2009; Lee et al., 2008). Transcripts that were significantly upregulated in the *Er71* mutant EYFP$^+$ cells compared with the *Er71* wild-type EYFP$^+$ cells were associated with muscle lineages (Fig. 4B). These transcripts included *Smarcd3*, *Myl3*, *Irx4*, *Tnni1*, *Myl2* and *Tbx5* (cardiac-restricted transcripts); *Acta1*, *Myl1*, *Svep1*, *Dpf3* and *Cdo1* (skeletal muscle-expressed transcripts); and *Acta2* and *Myl9* (vascular smooth muscle-specific transcripts). These results suggested that the EYFP$^+$ cells gave rise to other mesodermal lineages in the absence of ER71.

In order to determine whether the cardiac lineage was broadly affected, we analyzed transcripts from the cardiac development gene list in gene ontology (GO) terms and performed a hierarchical clustering analysis. Similar to the results obtained from whole-genome analysis, wild-type EYFP$^+$ cells segregated from the mutant EYFP$^+$ cells (and all EYFP$^-$ cells) (supplementary material Fig. S4A). This result demonstrated that the difference between these two populations can also be detected based only on cardiac development criteria. Some transcripts were decreased in EYFP$^+$ *Er71* mutant populations compared with EYFP$^+$ wild-type cells, including a number of transcripts that are important for endocardial development (including *Eng*, *Hhex*, *Sox18*, *Nfatc1*, *Sox17*) (supplementary material Fig. S4B). A number of transcripts were increased in expression in the EYFP$^+$ *Er71* mutant population compared with the other three groups (EYFP$^+$ wild-type and both EYFP$^-$ populations), including a number of cardiac transcription factors (*Myocd*, *Nkx2-5*, *Irx4*, *Isl1*, *Gata6*, *Tbx20*, *Tbx5*, *Gata4*, *Smyd1* and *Srf*) and structure-function transcripts (*Myl2*, *Myh7*, *Myl3*, *Tnnc1*, *Tnnt2*, *Tnni3*) (supplementary material Fig. S4C). We validated changes in selected transcripts by qPCR on independent samples and confirmed decreased expression of *Er71*, *Tal1* and *Cdh5* and the overexpression of cardiac transcripts including *Nkx2-5*, *Gata4* and *Tbx5* in *Er71* mutant EYFP$^+$ cells (Fig. 5).

In summary, our transcriptome analysis indicated that cardiac genes are over-represented in *Er71* mutant EYFP$^+$ cells, whereas endothelial, endocardial and hematopoietic genes are under-represented.

A novel *Er71-Cre* transgene marks endothelial and hematopoietic lineages

In order to determine whether ER71-expressing cells give rise to organs or programs other than the endothelial and hematopoietic lineages, we generated an *Er71-Cre* transgenic mouse model (Fig. 6A). We obtained a total of six founder lines, with embryos that showed similar expression patterns after breeding with the Rosa-

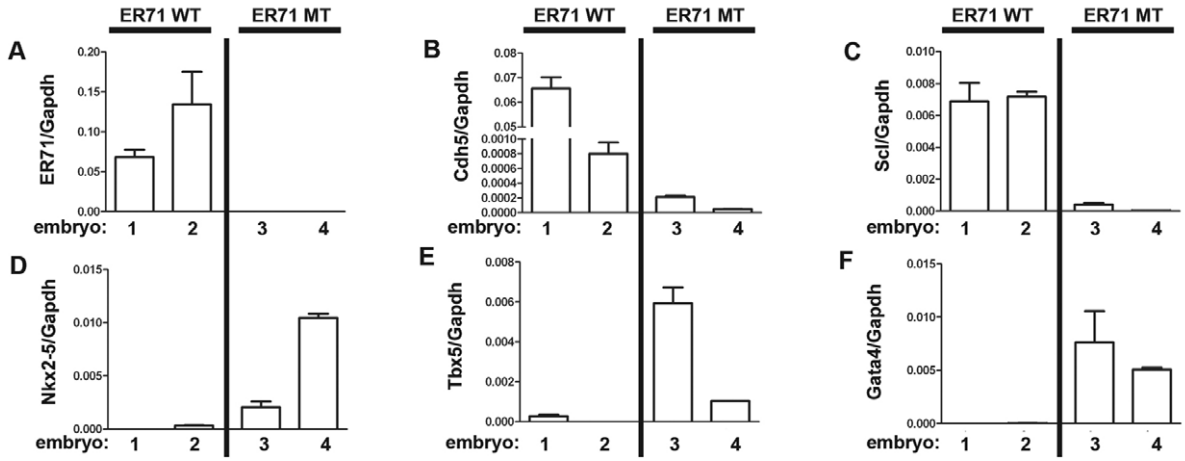

Fig. 5. Representative transcripts from the cardiac program are overexpressed in the *Er71* mutant. (**A-F**) qPCR analysis was performed on RNA isolated from EYFP$^+$ cells in the wild-type (embryos 1 and 2) and mutant (embryos 3 and 4) backgrounds. We observed the loss of *Er71* (A), *Cdh5* (B) and *Scl* (C) expression and an increase in the expression of representative cardiac program transcripts including *Nkx2-5* (D), *Tbx5* (E), and *Gata4* (F). Error bars indicate s.e.m.

lacZ reporter mice (supplementary material Fig. S5). Two transgenic lines were crossed to the Rosa-EYFP reporter mice and used for immunohistochemical and FACS analyses. Our results revealed that E11.5 embryos were marked by Rosa-EYFP or Rosa-lacZ in the endocardium, cardiac cushions, vasculature, mesenchyme and the fetal liver, which is the stage-appropriate site of hematopoiesis (Fig. 6B; supplementary material Fig. S5G,H; data not shown). Hearts of P3 neonates were marked by Rosa-EYFP in the vascular structures (Fig. 6C). Co-staining for EYFP and desmin, an early muscle-specific structural protein, showed that the Rosa-EYFP reporter did not overlap with desmin staining in the heart at either time point (Fig. 6B,C). FACS analysis of whole E11.5 embryos showed that 7-8% of cells in the E11.5 embryo were derived from ER71-expressing cells (Fig. 6D,E). Of these EYFP$^+$ cells, ~12% were endothelial (CD45$^-$ CD41$^-$ Tie2$^+$; Fig. 6F), 23% were non-erythroid hematopoietic cells (CD45$^+$, also

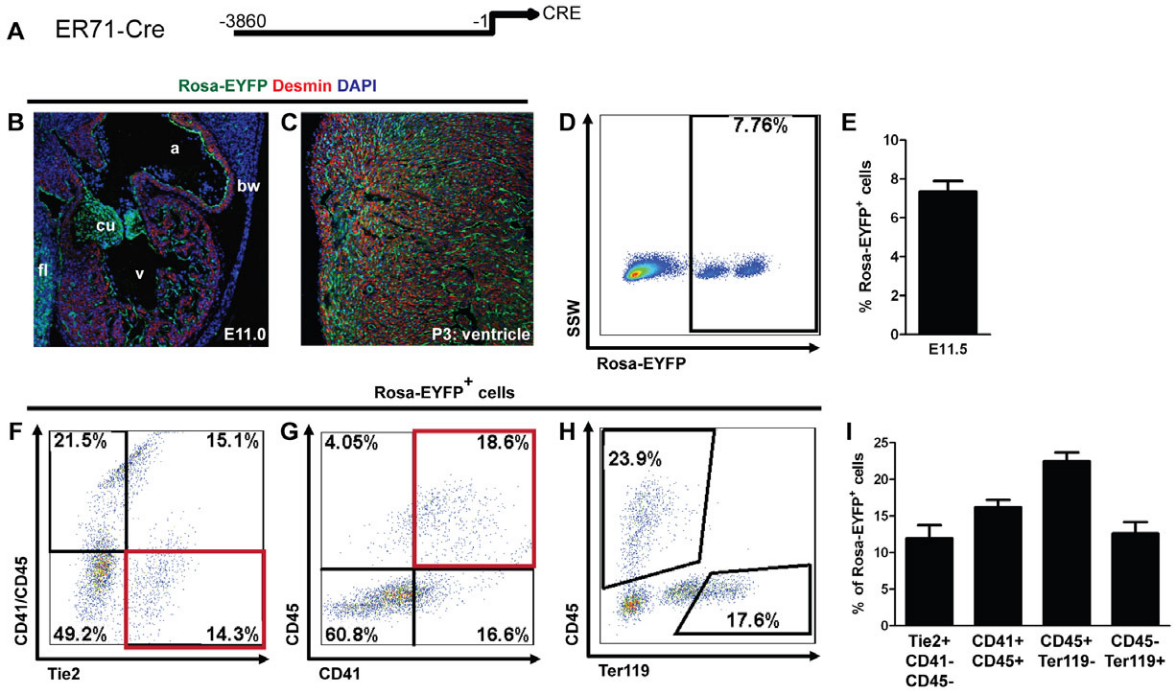

Fig. 6. Genetic fate-mapping studies indicate that ER71-expressing cells give rise to the endothelial and hematopoietic lineages. (**A**) The transgenic *Er71-Cre* mouse model used for these studies. (**B**,**C**) Immunohistochemistry for GFP (green) and desmin (red) and DAPI staining (blue) in E11.5 (B) and P3 (C) heart. a, atria; bw, body wall; cu, cardiac cushion; fl, fetal liver; v, ventricle. (**D**) A representative FACS profile showing EYFP$^+$ versus side scatter width (SSW). (**E**) Percentage of Rosa-EYFP$^+$ cells from all experiments (n=9). (**F-H**) EYFP-positive cells were gated and analyzed for lineage contribution. Representative FACS profiles are shown for (F) endothelial lineage (CD41$^-$ CD45$^-$ Tie2$^+$) cells and (G) CD41$^+$ CD45$^+$, (H) CD45$^+$ Ter119$^-$ and Ter119$^+$ CD45$^-$ hematopoietic lineage cells. (**I**) Percentage of Rosa-EYFP$^+$ cells of each lineage from all experiments (n=9). Error bars indicate s.e.m.

DEVELOPMENT

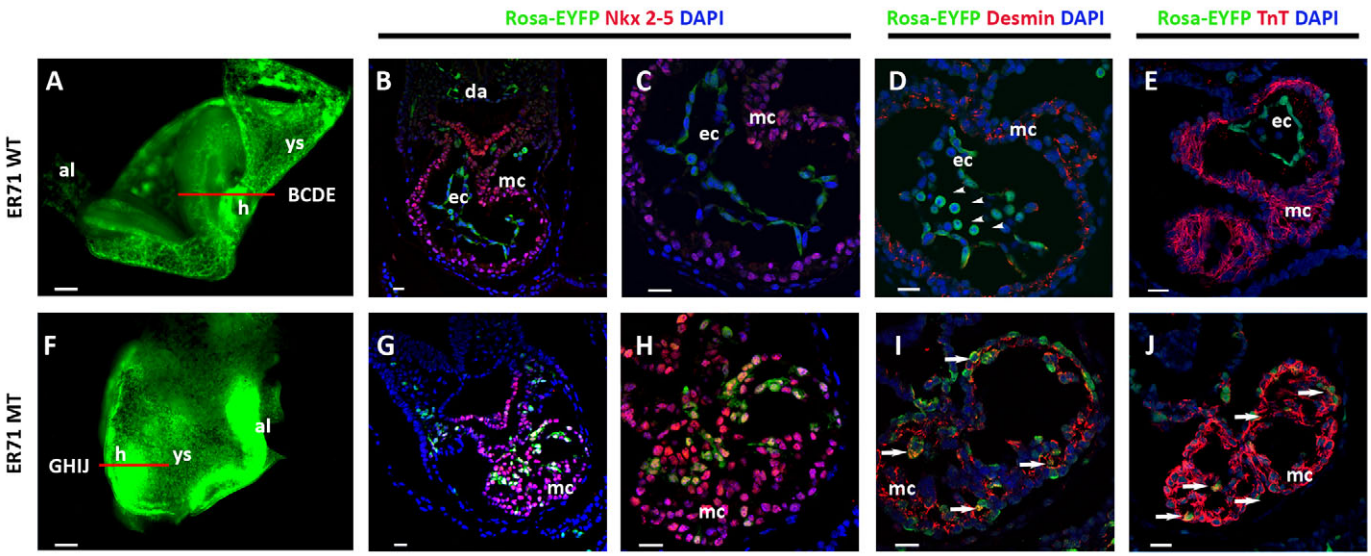

Fig. 7. Genetic fate-mapping studies in the *Er71* mutant show that the affected lineages give rise to myocardium in vivo. (**A**,**F**) Whole-mount images of Rosa-EYFP expression in *Er71* wild-type (A) and mutant (F) mouse embryos. The red line indicates the plane of sectioning for the corresponding panels. (**B**,**C**,**G**,**H**) Immunohistochemical analysis of EYFP and Nkx2-5 shown at low (B,G) and high (C,H) magnification. (**D**,**E**,**I**,**J**) Immunohistochemical analysis of EYFP and desmin (D,I) or troponin T (E,J) expression. ys, yolk sac; h, heart; al, allantois; da, dorsal aortae; ec, endocardium; mc, myocardium. Arrowheads indicate EYFP colocalization with desmin or troponin T. Scale bars: 200 μm in A,F; 20 μm in B-E,G-J.

known as Ptprc; Fig. 6H), and 13% were erythroid (Ter119$^+$; also known as Ly76; Fig. 6H). Interestingly, the EYFP$^+$ population segregated into two populations of varying EYFP expression (Fig. 6D). Ter119 primarily marked the EYFP-low population, whereas endothelial and other hematopoietic markers primarily marked the EYFP-high population (data not shown). This suggests that the Rosa reporters are expressed weakly in erythroid cells and might therefore inefficiently mark this population.

ER71-EYFP-expressing cells give rise to myocardium in the *Er71* mutant

To determine whether ER71 reporter-positive cells could produce alternative lineages in the *Er71* mutant, we crossed the *Er71-Cre* and *Rosa-EYFP* alleles into the *Er71* mutant background. As observed with the ER71-EYFP reporter, *Er71* mutants carrying the *Er71-Cre* and *Rosa-EYFP* alleles displayed altered EYFP expression patterns. Compared with the *Er71* wild-type embryos at E8.0, in which Rosa-EYFP is expressed in the yolk sac, vessels and heart tube (Fig. 7A), the *Er71* mutant embryos had robust EYFP expression localized in the allantois, posterior mesoderm and paraxial mesoderm (Fig. 7F). We speculate that the increased expression in the allantois and the posterior mesoderm is due to the progenitor cells differentiating to alternative mesodermal lineages, perturbed migration patterns, or a combination of the two. Embryos were analyzed using immunohistochemical techniques for co-expression of EYFP and Nkx2-5, a cardiac transcription factor, EYFP and desmin, or EYFP and troponin T, a cardiac sarcomeric protein. In wild-type hearts at E8.0, EYFP was expressed in the endocardium, the major vessels such as the dorsal aortae and in hematopoietic cells within the heart (Fig. 7B-E). There was no overlap of EYFP expression with Nkx2-5, desmin or troponin T.

In the *Er71* mutant embryo, the vessels and endocardium were absent. However, EYFP expression persisted in the heart. In the heart of the *Er71* mutant embryo, all EYFP-expressing cells had an Nkx2-5-positive nucleus (Fig. 7G,H). Some of the EYFP-expressing cells were also positive for the structural proteins desmin and troponin T (Fig. 7I,J, arrows). These results support the notion that the EYFP$^+$ cells are capable of differentiating to the myocardial lineage in the absence of ER71. It is likely that progenitor cell populations are also capable of differentiating toward other lineages depending on the context of the spatial and temporal cues that they are exposed to during embryogenesis. However, the heart is one of the few organs present at E8.0 and *Er71* mutant embryos are nonviable by E9.5. Therefore, the lethality of the *Er71* mutant limits our ability to evaluate the contribution of EYFP$^+$ progenitors to other lineages that develop later during embryogenesis.

ER71 overexpression suppresses development of the cardiac lineage

To complement our analysis of the *Er71* mutant embryo, we overexpressed ER71 using a doxycycline-inducible embryonic stem cell (ES)/EB system. An ES cell line in which expression of ER71 can be induced by doxycycline treatment was generated by a cassette exchange method (Iacovino et al., 2009). ES cells were induced to form EBs in differentiation media and cultured for 10 days with or without 0.5 mg/ml doxycycline from day 3. In the ER71-overexpressing EBs, we observed a decrease in the expression of troponin T, which we quantified by comparing the positively stained area with the total area of the EB (Fig. 8A-E). We also observed a decrease in cardiac gene expression (*Nkx2-5*, *Tbx5* and *Gata4*), as quantified by qPCR analyses (Fig. 8F). Finally, we quantitated the ability of the EBs to beat with edge detection. The doxycycline-induced EBs had a dramatic reduction in contractility (Fig. 8G) and in percent shortening (Fig. 8H). Collectively, these results further support the notion that ER71 suppresses the myocardial fate of mesodermal progenitors.

DISCUSSION

An array of signaling cascades and networks govern the fate of progenitor cell populations and their contribution to mesodermal lineages during embryogenesis. Recent studies have demonstrated

that various progenitors give rise to multiple mesodermal lineages. This broad developmental capacity is evident from the fact that multipotent progenitors have been shown to differentiate to diverse lineages, including hematopoietic, endothelial, cardiomyocyte and smooth muscle lineages. We have previously demonstrated that ER71, a member of the Ets transcription factor family, is essential for the development of mesodermal lineages. *Er71* mutant embryos lack hematopoietic and vascular lineages and are nonviable. Here, we have further defined the role of ER71 during mesodermal patterning and have made three new discoveries that advance our mechanistic understanding of mesodermal fate decisions during development.

First, we have defined the expression pattern of ER71 during embryogenesis using a newly generated transgenic reporter mouse model. Using immunohistochemical techniques, we demonstrated that ER71 is largely co-expressed with Tie2 in endothelial and hematopoietic progenitors. In the absence of ER71, we observed that these progenitors are expanded in number but do not represent the hematopoietic and endothelial lineages; rather, they are redirected to other mesodermal lineages, including the cardiac lineage. These data also show that ER71 is not required for the initiation or maintenance of its own expression. In the absence of ER71, this increase in the number of progenitors (EYFP$^+$ cells) might represent a delay in cell cycle withdrawal due to the lack of distinct mesodermal lineages (i.e. hematopoietic and endothelial lineages) or, alternatively, decreased programmed cell death involving these progenitors. We did not observe an increase in apoptosis in the *Er71* mutant embryo compared with its wild-type littermate control (Ferdous et al., 2009). Thus, we hypothesize that the progenitor cell expansion in the absence of ER71 is a result of the lack of cellular differentiation to hemato-endothelial lineages.

Our second discovery defined the fate of the ER71 progenitors in the presence and absence of ER71. Using genetic fate-mapping strategies, FACS and whole-genome analysis, we demonstrated that ER71 progenitors give rise to hematopoietic, endothelial and mesenchymal lineages. In the *Er71* mutant background, these progenitors (EYFP$^+$ cells) produced other mesodermal lineages, including the cardiomyocyte lineage (supplementary material Fig. S6). Moreover, our FACS and transcriptome data supported the notion that paraxial mesodermal programs (transcripts enriched in the skeletal muscle lineage) were increased in the *Er71* mutant progenitors. Accumulating evidence suggests that the cardiac and hematopoietic lineages develop from a common progenitor and that the specification of these lineages is inversely regulated. We recently demonstrated that Nkx2-5 has a dual transcriptional regulatory role during embryogenesis as it represses Gata1-mediated hematopoiesis and promotes cardiogenesis of the multipotent mesodermal progenitors (Caprioli et al., 2011). The results of the present study further support the plasticity of the ER71 progenitors and their capacity to respond to cues and contribute to other mesodermal lineages.

The origin of endocardium relative to the myocardium has been controversial (Harris and Black, 2010). Studies in zebrafish and chick suggest that endocardial and myocardial lineages are distinct from the point of gastrulation, and there are no multipotent progenitors (Cohen-Gould and Mikawa, 1996; Wei and Mikawa, 2000). By contrast, lineage-tracing studies in mouse embryos and ES cells suggest that endocardial progenitors are specified as multipotent progenitors in the cardiac crescent and cell fate is later specified to either endocardial, myocardial or vascular smooth muscle fates

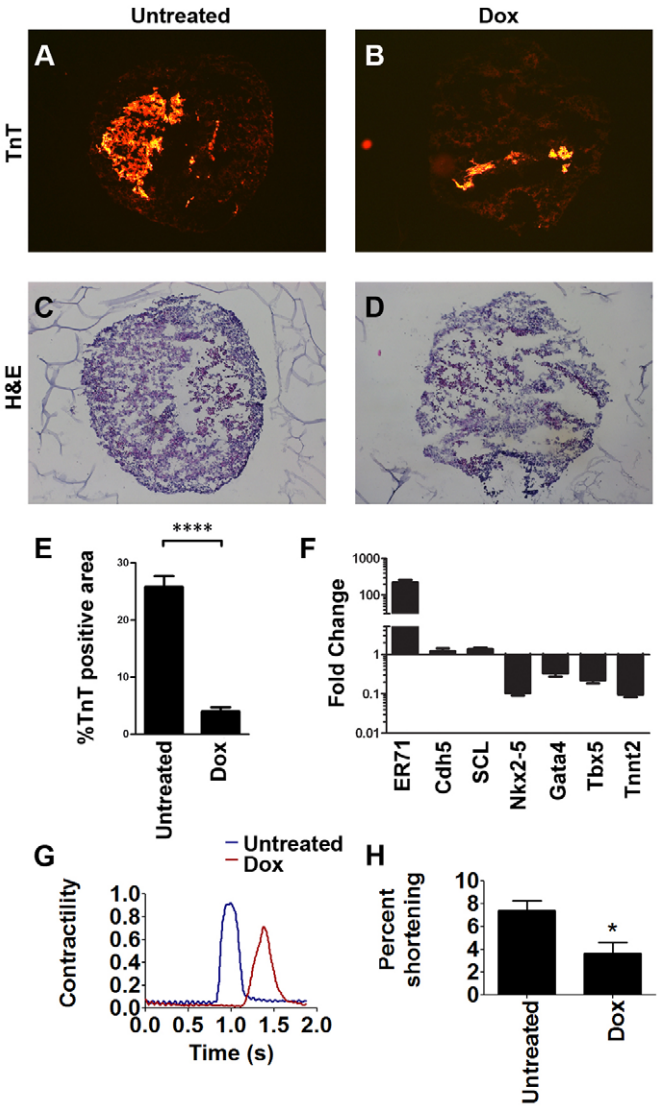

Fig. 8. Overexpression of ER71 in differentiating EBs inhibits cardiac development. (**A-D**) Sections of representative EBs either untreated (A,C) or induced to overexpress ER71 (B,D) stained with Hematoxylin and Eosin (C,D) or anti-TnT (A,B). (**E**) Quantitative analysis of the troponin T-positive area in 33 induced (Dox) and 42 untreated sections. (**F**) qRT-PCR confirms that representative cardiac program transcripts (*Nkx2-5*, *Tbx5*, *Gata4*) are downregulated in ER71-overexpressing EBs. (**G**,**H**) Extent of contraction and relaxation after 2 seconds of stimulation (G) and percent shortening (H) are reduced in ER71-overexpressing EBs. ****, $P<0.001$; *, $P<0.05$. Error bars indicate s.e.m.

(Kattman et al., 2006; Misfeldt et al., 2009). In our novel ER71-EYFP reporter mice, we observed weak co-expression of Nkx2-5 protein and EYFP in the cardiac crescent at E7.75. However, lineage-tracing experiments showed that cells that expressed ER71 during any point in their development did not become cardiomyocytes. By contrast, Nkx2-5-Cre lineage-tracing experiments show that at least some of the endocardial lineage derives from cells that expressed Nkx2-5 (Stanley et al., 2002). Taken together, these observations favor a model in which common progenitors of endocardial and myocardial lineages are specified as Nkx2-5$^+$ cells in the cardiac crescent, but those that

will become endocardium will downregulate myocardial potential, including the expression of Nkx2-5. Once ER71 is expressed, the fate is restricted to endocardium, and not myocardial lineages. Future studies are warranted to decipher the mechanism that governs the specification of endocardial cells within the cardiac progenitor pool.

Our third finding is that ER71 overexpression repressed cardiac potential. These results support the notion that ER71, like Nkx2-5, has reciprocal and overlapping dual roles in the specification of mesodermal lineages. Our previous studies demonstrated that Nkx2-5 overexpression suppressed hematopoiesis, but not the endothelial program (Caprioli et al., 2011). We further defined that Nkx2-5 could, in a context-dependent fashion, transcriptionally activate *Er71* and promote endocardial lineage development (Ferdous et al., 2009). Collectively, our previous studies and recent results support the notion that distinct transcriptional networks can, in a context-dependent fashion (and dependent on the local environment), activate a hematopoietic or endothelial program and antagonize the cardiac program. These studies further emphasize the plasticity of progenitors and their contribution to distinct lineages.

In summary, our data support a dual role for ER71 in the specification of the endothelial and hematopoietic lineages and the suppression of other lineages (i.e. myocardial and paraxial mesodermal cell fates) (supplementary material Fig. S6). Our studies further support the notion of multipotent mesodermal progenitors that are dependent on transcriptional cascades and other cues to direct them to populate one or more lineages. Moreover, our studies reveal that global deletion of a single gene (i.e. *Er71*) aborts one or more lineages and redirects the cells to other lineages that would not typically arise from those progenitors. These studies further our understanding of the regulatory mechanisms that govern mesodermal cell fate decisions and embryogenesis.

Acknowledgements
We thank Jennifer L. Springsteen and Alicia M. Wallis for assistance with histological analyses and animal care.

Funding
Funding support was obtained from the National Institutes of Health [U01 HL100407 and R01 HL085729 to D.J.G.]; and the American Heart Association [Jon Holden DeHaan Foundation 0970499 to D.J.G.]. Deposited in PMC for release after 12 months.

Competing interests statement
The authors declare no competing financial interests.

Supplementary material
Supplementary material available online at
http://dev.biologists.org/lookup/suppl/doi:10.1242/dev.070912/-/DC1

References
Benjamini, Y. and Hochberg, Y. (1995). Controlling the false discovery rate: a practical and powerful approach to multiple testing. *J. R. Statist. Soc. B* **97**, 289-300.
Bondue, A., Tannler, S., Chiapparo, G., Chabab, S., Ramialison, M., Paulissen, C., Beck, B., Harvey, R. and Blanpain, C. (2011). Defining the earliest step of cardiovascular progenitor specification during embryonic stem cell differentiation. *J. Cell Biol.* **192**, 751-765.
Caprioli, A., Koyano-Nakagawa, N., Iacovino, M., Shi, X., Ferdous, A., Harvey, R. P., Olson, E. N., Kyba, M. and Garry, D. J. (2011). Nkx2-5 represses Gata1 gene expression and modulates the cellular fate of cardiac progenitors during embryogenesis. *Circulation* **123**, 1633-1641.
Carbon, S., Ireland, A., Mungall, C. J., Shu, S., Marshall, B. and Lewis, S. (2009). AmiGO: online access to ontology and annotation data. *Bioinformatics* **25**, 288-289.
Cohen-Gould, L. and Mikawa, T. (1996). The fate diversity of mesodermal cells within the heart field during chicken early embryogenesis. *Dev. Biol.* **177**, 265-273.
Davis, L. A. and Zur Nieden, N. I. (2008). Mesodermal fate decisions of a stem cell: the Wnt switch. *Cell Mol. Life Sci.* **65**, 2658-2674.
de Hoon, M. J., Imoto, S., Nolan, J. and Miyano, S. (2004). Open source clustering software. *Bioinformatics* **20**, 1453-1454.
De Val, S., Chi, N. C., Meadows, S. M., Minovitsky, S., Anderson, J. P., Harris, I. S., Ehlers, M. L., Agarwal, P., Visel, A., Xu, S. M. et al. (2008). Combinatorial regulation of endothelial gene expression by ets and forkhead transcription factors. *Cell* **135**, 1053-1064.
Downs, K. M. and Davies, T. (1993). Staging of gastrulating mouse embryos by morphological landmarks in the dissecting microscope. *Development* **118**, 1255-1266.
Dumont, D. J., Yamaguchi, T. P., Conlon, R. A., Rossant, J. and Breitman, M. L. (1992). tek, a novel tyrosine kinase gene located on mouse chromosome 4, is expressed in endothelial cells and their presumptive precursors. *Oncogene* **7**, 1471-1480.
Ema, M., Takahashi, S. and Rossant, J. (2006a). Deletion of the selection cassette, but not cis-acting elements, in targeted Flk1-lacZ allele reveals Flk1 expression in multipotent mesodermal progenitors. *Blood* **107**, 111-117.
Ema, M., Yokomizo, T., Wakamatsu, A., Terunuma, T., Yamamoto, M. and Takahashi, S. (2006b). Primitive erythropoiesis from mesodermal precursors expressing VE-cadherin, PECAM-1, Tie2, endoglin and CD34 in the mouse embryo. *Blood* **108**, 4018-4024.
Ferdous, A., Caprioli, A., Iacovino, M., Martin, C. M., Morris, J., Richardson, J. A., Latif, S., Hammer, R. E., Harvey, R. P., Olson, E. N. et al. (2009). Nkx2-5 transactivates the Ets-related protein 71 gene and specifies an endothelial/endocardial fate in the developing embryo. *Proc. Natl. Acad. Sci. USA* **106**, 814-819.
Harris, I. S. and Black, B. L. (2010). Development of the endocardium. *Pediatr. Cardiol.* **31**, 391-399.
Iacovino, M., Hernandez, C., Xu, Z., Bajwa, G., Prather, M. and Kyba, M. (2009). A conserved role for Hox paralog group 4 in regulation of hematopoietic progenitors. *Stem Cells Dev.* **18**, 783-792.
Irizarry, R. A., Hobbs, B., Collin, F., Beazer-Barclay, Y. D., Antonellis, K. J., Scherf, U. and Speed, T. P. (2003). Exploration, normalization and summaries of high density oligonucleotide array probe level data. *Biostatistics* **4**, 249-264.
Ivey, K. N., Muth, A., Arnold, J., King, F. W., Yeh, R. F., Fish, J. E., Hsiao, E. C., Schwartz, R. J., Conklin, B. R., Bernstein, H. S. et al. (2008). MicroRNA regulation of cell lineages in mouse and human embryonic stem cells. *Cell Stem Cell* **2**, 219-229.
Kataoka, H., Takakura, N., Nishikawa, S., Tsuchida, K., Kodama, H., Kunisada, T., Risau, W., Kita, T. and Nishikawa, S. I. (1997). Expressions of PDGF receptor alpha, c-Kit and Flk1 genes clustering in mouse chromosome 5 define distinct subsets of nascent mesodermal cells. *Dev. Growth Differ.* **39**, 729-740.
Kattman, S. J., Huber, T. L. and Keller, G. M. (2006). Multipotent flk-1+ cardiovascular progenitor cells give rise to the cardiomyocyte, endothelial and vascular smooth muscle lineages. *Dev. Cell* **11**, 723-732.
Kaufman, M. H. (1992). *The Atlas of Mouse Development*. London: Academic Press.
Kennedy, M., Firpo, M., Choi, K., Wall, C., Robertson, S., Kabrun, N. and Keller, G. (1997). A common precursor for primitive erythropoiesis and definitive haematopoiesis. *Nature* **386**, 488-493.
Kisanuki, Y. Y., Hammer, R. E., Miyazaki, J., Williams, S. C., Richardson, J. A. and Yanagisawa, M. (2001). Tie2-Cre transgenic mice: a new model for endothelial cell-lineage analysis in vivo. *Dev. Biol.* **230**, 230-242.
Lee, D., Park, C., Lee, H., Lugus, J. J., Kim, S. H., Arentson, E., Chung, Y. S., Gomez, G., Kyba, M., Lin, S. et al. (2008). ER71 acts downstream of BMP, Notch and Wnt signaling in blood and vessel progenitor specification. *Cell Stem Cell* **2**, 497-507.
Li, W., Ferkowicz, M. J., Johnson, S. A., Shelley, W. C. and Yoder, M. C. (2005). Endothelial cells in the early murine yolk sac give rise to CD41-expressing hematopoietic cells. *Stem Cells Dev.* **14**, 44-54.
Misfeldt, A. M., Boyle, S. C., Tompkins, K. L., Bautch, V. L., Labosky, P. A. and Baldwin, H. S. (2009). Endocardial cells are a distinct endothelial lineage derived from Flk1+ multipotent cardiovascular progenitors. *Dev. Biol.* **333**, 78-89.
Moretti, A., Caron, L., Nakano, A., Lam, J. T., Bernshausen, A., Chen, Y., Qyang, Y., Bu, L., Sasaki, M., Martin-Puig, S. et al. (2006). Multipotent embryonic isl1+ progenitor cells lead to cardiac, smooth muscle and endothelial cell diversification. *Cell* **127**, 1151-1165.
Motoike, T., Markham, D. W., Rossant, J. and Sato, T. N. (2003). Evidence for novel fate of Flk1+ progenitor: contribution to muscle lineage. *Genesis* **35**, 153-159.
Omelyanchuk, N., Orlovskaya, I. A., Schraufstatter, I. U. and Khaldoyanidi, S. K. (2009). Key players in the gene networks guiding ESCs toward mesoderm. *J. Stem Cells* **4**, 147-160.
Park, M., Yaich, L. E. and Bodmer, R. (1998). Mesodermal cell fate decisions in Drosophila are under the control of the lineage genes numb, Notch and sanpodo. *Mech. Dev.* **75**, 117-126.

Sarb, S., Cimpean, A. M. and Grigoras, D. (2010). Tie2 expression in human embryonic tissues. *Rom. J. Morphol. Embryol.* **51**, 81-84.

Schlaeger, T. M., Bartunkova, S., Lawitts, J. A., Teichmann, G., Risau, W., Deutsch, U. and Sato, T. N. (1997). Uniform vascular-endothelial-cell-specific gene expression in both embryonic and adult transgenic mice. *Proc. Natl. Acad. Sci. USA* **94**, 3058-3063.

Schnurch, H. and Risau, W. (1993). Expression of tie-2, a member of a novel family of receptor tyrosine kinases, in the endothelial cell lineage. *Development* **119**, 957-968.

Smyth, G. (2005). limma: linear models for microarray data. In *Bioinformatics and Computational Biology Solutions Using R and Bioconductor* (ed. V. J. C. Robert Gentleman, W. Huber, R. A. Irizarry and S. Dudoit), pp. 397-420. New York: Springer.

Stanley, E. G., Biben, C., Elefanty, A., Barnett, L., Koentgen, F., Robb, L. and Harvey, R. P. (2002). Efficient Cre-mediated deletion in cardiac progenitor cells conferred by a 3′UTR-ires-Cre allele of the homeobox gene Nkx2-5. *Int. J. Dev. Biol.* **46**, 431-439.

Takakura, N., Yoshida, H., Ogura, Y., Kataoka, H. and Nishikawa, S. (1997). PDGFR alpha expression during mouse embryogenesis: immunolocalization analyzed by whole-mount immunohistostaining using the monoclonal anti-mouse PDGFR alpha antibody APA5. *J. Histochem. Cytochem.* **45**, 883-893.

Wei, Y. and Mikawa, T. (2000). Fate diversity of primitive streak cells during heart field formation in ovo. *Dev. Dyn.* **219**, 505-513.

Wu, S. M., Fujiwara, Y., Cibulsky, S. M., Clapham, D. E., Lien, C. L., Schultheiss, T. M. and Orkin, S. H. (2006). Developmental origin of a bipotential myocardial and smooth muscle cell precursor in the mammalian heart. *Cell* **127**, 1137-1150.